PLL-Free Synchronous QPSK Polarization Multiplex/Diversity Receiver Concept With Digital I&Q Baseband Processing

R. Noé

***Abstract*—This synchronous quadrature-phase-shift keying (QPSK) receiver concept allows us to process signals in parallel after electronic demultiplexing. An automatic electronic polarization control with a control time constant in the low microsecond range is provided. It is followed by a phase-locked loop free carrier recovery. An intermediate frequency linewidth tolerance of up to 10^{-3} times the QPSK symbol rate is expected. Commercially available distributed feedback lasers shall, therefore, suffice.**

***Index Terms*—Homodyne detection, optical fiber communication, phase-shift keying, quadrature-phase-shift keying (QPSK), synchronous detection.**

I. Introduction

QUADRATURE-PHASE-SHIFT keying (QPSK)-based multilevel modulation formats promise ultimate performance and dispersion tolerance in upgraded or newly built fiber links. Differential QPSK receivers [1]–[4] suffer from a 2.3-dB sensitivity penalty compared to synchronous QPSK receivers and require optical polarization control if both interferometric detection and polarization-division multiplex are used [2].

Coherent optical polarization diversity receivers permit a fully electronic polarization control [5], [6]. Equalization of distortions caused by polarization-mode dispersion (PMD) and chromatic dispersion is likewise possible. A phase-locked loop (PLL)-based carrier recovery for synchronous QPSK transmission would fail in combination with distributed feedback (DFB) lasers because the product of laser linewidth times loop delay is too large [7], [8]. An analog phase noise tolerant feedforward carrier recovery concept has been presented in [9] for a coherent in-phase and quadrature (I&Q), synchronous QPSK receiver. An intermediate frequency (IF) linewidth tolerance of up to 10^{-3} times the symbol rate was predicted with additional polarization-division multiplex. Digital processing of the QPSK signals is also possible [10].

In this letter, it will be shown how a penalty-free electronic polarization control can be integrated into such a scheme, and operated with a control time constant in the low microsecond range. A key application is the upgrading of existing 10 Gb/s links to 40 Gb/s.

Manuscript received October 29, 2004; revised November 25, 2004. This work was supported by the European Commission under Contract 004631 in FP6 IST-2002-2.3.2.2.

The author is with the University Paderborn, EIM-E, Optical Communication and High Frequency Engineering, D-33098 Paderborn, Germany (e-mail: noe@upb.de).

Digital Object Identifier 10.1109/LPT.2004.842795

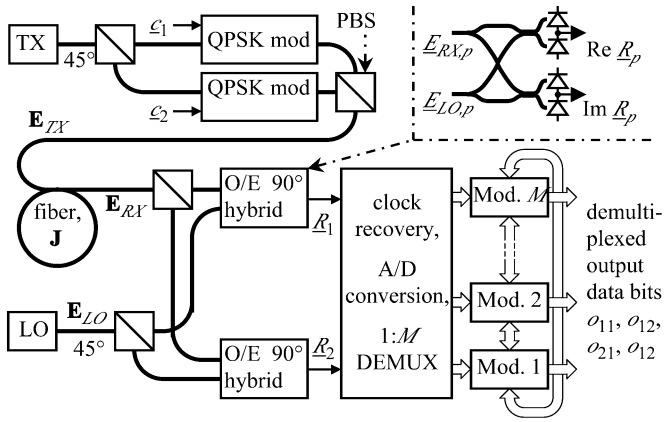

Fig. 1. Polarization multiplexed synchronous QPSK transmission system with digital receiver. Inset: Optoelectronic 90° hybrid.

TABLE I
Bipolar Bits versus Quadrant Number

d_{p1}, Re $\underline{c}_p$, Re $\underline{r}_p$, o_{p1}	d_{p2}, Im $\underline{c}_p$, Im $\underline{r}_p$, o_{p2}	$n_{d,p}$, $n_{c,p}$, $n_{r,p}$, $n_{o,p}$
1	1	0
-1	1	1
-1	-1	2
1	-1	3

II. Transmission System

Fig. 1 shows a QPSK polarization-division-multiplex transmission system. The transmitter laser (TX) signal is split, QPSK-modulated in two branches, and recombined with two $(p = 1, 2)$ orthogonal polarizations in a polarization beam splitter. Two bipolar data bits d_{p1}, d_{p2} are to be transmitted in each polarization, four per symbol in total. d_{p1}, d_{p2} are Gray-encoded into a data quadrant number $n_{d,p}$ (Table I). It is differentially encoded to form an encoded quadrant number $n_{c,p}$ with $n_{c,p}(i) = (n_{d,p}(i) + n_{c,p}(i-1)) \bmod 4$. This number defines the quadrant of the transmitted complex symbol $\underline{c}_p = \mathrm{Re}\,\underline{c}_p + j\,\mathrm{Im}\,\underline{c}_p = \pm 1 \pm j$ ($p = 1, 2$; Table I), the real and imaginary parts of which drive the respective QPSK modulator.

The transmitted electric field $\mathbf{E}_{\mathrm{TX}}$ is proportional to the vector $\mathbf{c} = [\underline{c}_1\ \underline{c}_2]^T$. The received electric field $\mathbf{E}_{\mathrm{RX}} = \mathbf{J}\mathbf{E}_{\mathrm{TX}}$ has been multiplied by the fiber Jones matrix $\mathbf{J}$.

The receiver features a 45°-polarized local oscillator (LO) laser. Received and LO signals are each split into orthogonal polarizations, and the fields $\underline{E}_{\mathrm{RX},p}, \underline{E}_{\mathrm{LO},p}$ of each polarization p are detected in optoelectronic 90° hybrids (inset of Fig. 1). The

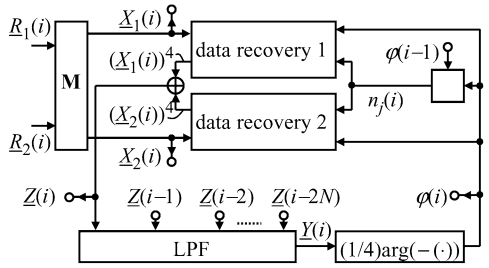

Fig. 2. Block diagram of kth ($k = i \bmod M$) digital signal processing module after the demultiplexer. Here and in Fig. 3, the inputs and outputs terminated by a circle may or must interface with other modules for carrier recovery.

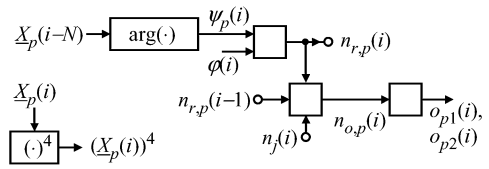

Fig. 3. Block diagram of "data recovery p" (polarization $p = 1, 2$). Signal $\underline{X}_p(i-N)$ is provided by another (not the kth) module. $n_{r,p}(i), n_{r,p}(i-1)$ assure communication between data recoveries of neighbor modules. $o_{p1}(i), o_{p2}(i)$ are output data bits (Fig. 1).

I&Q signals can be understood to be real and imaginary parts $\mathrm{Re}\,\underline{R}_p, \mathrm{Im}\,\underline{R}_p$ of a complex received IF signal $\underline{R}_p$, and these form together a received IF signal vector $\mathbf{R} = [\underline{R}_1\ \underline{R}_2]^T = \mathbf{J}\cdot\mathbf{c}\cdot e^{j\varphi''}$. Angle φ'' is the phase difference between signal and LO lasers. The IF is chosen to be near or at zero.

III. Carrier and Data Recovery

The clock can be recovered in an extra intensity modulation direct detection receiver or from the electrical I&Q signals. After clock recovery the I&Q signals of both polarization branches are sampled at the symbol rate, digitized and demultiplexed 1:M to a low symbol rate where complex digital functions can be implemented in complimentary metal–oxide–semiconductor (CMOS). The M data streams are processed in M modules (Mod). The modules also have to communicate among each other, as indicated by the inputs and outputs terminated by circles in Figs. 2 and 3. The ith vector sample $\mathbf{R}$ enters the kth module (Fig. 2), where $k = i \bmod M$. It is multiplied by a complex Jones matrix $\mathbf{M}$ to form a polarization-separated IF vector sample $\mathbf{X}(i) = [\underline{X}_1(i)\ \underline{X}_2(i)]^T = \mathbf{M}\mathbf{R}(i)$. Ideally, $\mathbf{M}\mathbf{J}$ is proportional to the unity matrix and it holds $\mathbf{X} = \mathbf{c}\cdot e^{j\varphi'}$. Angle $\varphi' - \varphi''$ is the phase shift introduced by the matrix product $\mathbf{M}\mathbf{J}$.

The components $\underline{X}_p$ ($p = 1, 2$) are processed in data recoveries (Fig. 3). Sample $\underline{X}_p(i)$ is raised to the fourth power. Due to $\underline{c}_p^4 = -4$, the modulation is thereby eliminated [9]. The resulting frequency-quadrupled carrier components $\underline{X}_p^4 \propto -e^{j4\varphi'}$ of both polarizations are added, $\underline{Z} = \underline{X}_1^4 + \underline{X}_2^4 \propto -e^{j4\varphi'}$. A further noise suppression results from a filtering of $\underline{Z}$ in a lowpass filter because the IF is at or near zero. A good filter may take the sum $\underline{Y}(i) = \sum_{m=0}^{2N} \underline{Z}_p(i-m)$ of the $2N+1$ most recent samples of the frequency-quadrupled carrier $\underline{Z}$. Most of them come from adjacent modules. The group delay in this filter (LPF) equals N symbols. $N = 2$ is a fairly good choice [9].

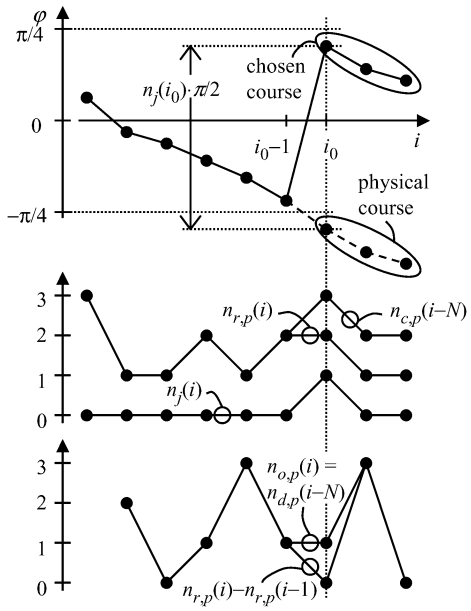

Fig. 4. Quadrant phase jump, its detection, and successful correction.

The filter also alters the phase angle. $\underline{Y} \propto -e^{j4\varphi}$ holds, where $4\varphi(i)$ would ideally be equal to $4\varphi'(i-N)$. The next step is to divide phase and frequency of $\underline{Y}$ by a factor of four in order to recover the carrier phase. The best choice is probably a two-dimensional lookup table which calculates carrier phase samples $\varphi(i) = (1/4)\arg(-\underline{Y}(i))$.

In each of the data recoveries ($p = 1, 2$), the phase angle $\psi_p(i) = \arg \underline{X}_p(i-N)$ of the received signal is calculated, with a delay equal to that experienced in the lowpass filter. For demodulation, an integer $n_{r,p}(i)$ which fulfills $n_{r,p}(i)\pi/2 \le \psi_p(i) - \varphi_p(i) < (n_{r,p}(i)+1)\pi/2$ is simply determined. It may be called a received quadrant number because $\underline{n}_{r,p}(i) = n_{c,p}(i-N)$ holds for $|\varphi(i) - \varphi'(i-N)| < \pi/4$.

There is a four-fold ambiguity in the calculation of $\varphi(i)$, and $n_{r,p}(i)$ does not, therefore, contain all needed information. Choosing $\varphi(i)$ as close as possible to $\varphi(i-1)$ could solve the problem but is practically impossible because the correct quadrant cannot be selected within one symbol duration. Instead, let $|\varphi(i)| \le \pi/4$ be always chosen. For correction of arising errors, the kth module must detect whether φ has jumped by an integer multiple of $\pi/2$. It determines a quadrant jump number $n_j(i)$ for this purpose. This is an integer which fulfills $|\varphi(i) - \varphi(i-1) - n_j(i)\pi/2| < \pi/4$. All quadrant numbers and operations are understood to be valid modulo 4 because the angle functions are periodic. Fig. 4 shows a quadrant phase jump at $i = i_0$ and its detection. The value $n_j(i_0) \neq 0$ indicates that all $n_{r,p}(i_+)$ with $i_+ \ge i_0$ carry an unwanted offset $-n_j(i_0)$. It is not possible to correct all $n_{r,p}(i_+)$ accordingly because this would have to be done at the symbol rate. But the differential quadrant encoding at the transmitter side allows us to calculate an output quadrant number $n_{o,p}(i) = (n_{r,p}(i) - n_{r,p}(i-1) + n_j(i)) \bmod 4 = n_{d,p}(i-N)$. It is identical to the delayed data quadrant number, and it yields the output data bits $o_{p1}(i), o_{p2}(i)$ (Table I). These are equal to the delayed data bits $d_{p1}(i-N), d_{p2}(i-N)$. The successful correction of the quadrant jump at $i = i_0$ is illustrated in the bottom of Fig. 4.

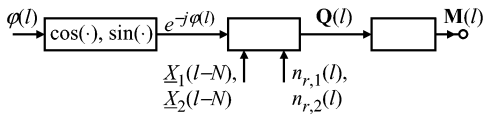

Fig. 5. Updating of the polarization control matrix $\mathbf{M}$.

IV. Electronic Polarization Control

The coefficients of the polarization control matrix $\mathbf{M}$ can and should be the same in all modules, but they must be updated to track changes of $\mathbf{J}$. If a perfect estimate $\langle\mathbf{Q}\rangle$ of the matrix product $\mathbf{MJ}$ is available, polarization can be controlled electronically and penalty-free by applying the iterative formula $\mathbf{M} := \langle\mathbf{Q}\rangle^{-1}\mathbf{M}$ (zero-forcing algorithm). For $\langle\mathbf{Q}\rangle \to \mathbf{1}$, where $\mathbf{1}$ is the unity matrix, the inverse can be approximated by $\langle\mathbf{Q}\rangle^{-1} = (\mathbf{1} - (\mathbf{1} - \langle\mathbf{Q}\rangle))^{-1} \approx \mathbf{1} + (\mathbf{1} - \langle\mathbf{Q}\rangle)$. In practice, it is, therefore, allowed to set $\mathbf{M} := (\mathbf{1} + (\mathbf{1} - \langle\mathbf{Q}\rangle))\mathbf{M}$.

An unknown matrix $\mathbf{N}$ can be estimated by correlating an input vector $\mathbf{A}$ having independent zero-mean elements with the output vector $\mathbf{NA}$: $\langle\mathbf{N}\rangle = \langle(\mathbf{NA})\mathbf{A}^{+}\rangle$. Matrix $\mathbf{Q}$ is obtained as follows: The polarization-separated IF vector is multiplied by $e^{-j\varphi}$ to get rid of phase noise. The result contains phase jumps and is differentially coded. Therefore, it must be correlated not with the recovered data itself but with the received data vector $\mathbf{r} = [\underline{r}_1\ \underline{r}_2]^T$ whose elements are defined in Table I by the received quadrant numbers $n_{r,p}$ (defined in Section III): $\mathbf{Q}(i) = (1/2) \cdot \mathbf{X}(i - N) \cdot e^{-j\varphi(i)} \cdot \mathbf{r}(i)^{+}$. The factor $1/2$ is not of importance; it merely assures $|\det(\mathbf{MJ})| \to 1$.

Better than waiting for a perfect estimate $\langle\mathbf{Q}\rangle$ is it to choose a low control gain $g \ll 1$ and to update $\mathbf{M}$ immediately as $\mathbf{M} := (\mathbf{1} + g(\mathbf{1} - \mathbf{Q}))\mathbf{M}$. System simulations in the presence of polarization-dependent loss and with random start values always correctly recover the carrier and $\mathbf{M}$, and indicate that $g = 10^{-4}$ is adequate. PMD affects the finding of $\mathbf{M}$ no more than the data. To allow for realtime operation, the $\mathbf{Q}(i)$ may be accumulated before an updating step of $\mathbf{M}$ is undertaken.

The control time constant equals roughly $1/g$ updating intervals. Since the symbol duration is so short, it should be sufficient in most applications to base the updating of $\mathbf{M}$ on matrices $\mathbf{Q}$ obtained in only one of the M signal processing modules. This reduces silicon floorspace. The calculations can be cast into the blocks of Fig. 5. These must be added in one of the signal processing modules. Index l is the M-fold subsampled symbol index at which the chosen module is clocked. The associated control time constant is M/g symbol durations, e.g., 16 μs for 10-Gbaud operation, $g = 10^{-4}$, and $M = 16$.

In principle, the updating of $\mathbf{M}$ also recovers the carrier, but the practical contribution of $\mathbf{M}$ to carrier recovery is negligible because the updating is slow. Imbalance of the 90° hybrid and similar effects can be corrected if $\mathbf{M}$ is replaced by a complex 2×4 matrix with the four real-valued input signals $\mathrm{Re}\,\underline{R}_1, \mathrm{Im}\,\underline{R}_1, \mathrm{Re}\,\underline{R}_2, \mathrm{Im}\,\underline{R}_2$. Only the number of coefficients increases, not the needed computation power.

V. Discussion

Each module processes only signals which are already available, and each processing step may include an arbitrary delay which just adds to the overall transmission delay but does not impede realtime operation. Regarding phase noise, the obtained tolerance is as good as if all processing took place at the symbol rate because the computations are identical. The function of the analog feedforward carrier recovery [9] is completely emulated, which means that the laser linewidth/symbol rate ratio can be up to 10^{-3}. At least $1/3$ of this can be realized experimentally, as may be concluded from a comparison of [9] with the experiment [11]. At 10 Gbaud, laser linewidths of $>$1.5 MHz should be tolerable at a bit-error rate $= 10^{-9}$, and more if forward-error correction is present.

VI. Conclusion

This digital feedforward carrier recovery scheme for QPSK is predicted to be extremely laser linewidth tolerant, just like its analog counterpart. As a consequence, synchronous QPSK becomes feasible even at 10 Gsymbols/s with commercially available DFB lasers and a digital coherent I&Q receiver. An important feature is a fast electronic polarization control, which has been shown to be fully compatible with the digital signal processing scheme.

References

[1] C. Wree *et al.*, "High spectral efficiency 1.6-b/s/Hz transmission (8 × 40 Gb/s with 25-GHz grid) over 200 km SSMF using RZ-DQPSK and polarization multiplexing," *IEEE Photon. Technol. Lett.*, vol. 15, no. 9, pp. 1303–1305, Sep. 2003.

[2] A. F. A. Ismail, D. Sandel, A. Hidayat, B. Milivojevic, S. Bhandare, H. Zhang, and R. Noé, "2.56 Tbit/s, 1.6 bit/s/Hz, 40 Gbaud RZ-DQPSK polarization division multiplex transmission over 273 km of fiber," in *OECC/COIN 2004*, Yokohama, Japan, Jul. 12–16, 2004, Paper PD1-4.

[3] A. H. Gnauck *et al.*, "Spectrally efficient (0.8 b/s/Hz) 1-Tb/s (25 × 42.7 Gb/s) RZ-DQPSK transmission over 28 100-km SSMF spans with 7 optical add/drops," in *Proc. ECOC 2004*, Stockholm, Sweden, Paper Th4.4.1.

[4] N. Yoshikane and I. Morita, "160% spectrally-efficient 5.12 Tb/s (64 × 85.4 Gb/s RZ DQPSK) transmission without polarization demultiplexing," in *Proc. ECOC 2004*, Stockholm, Sweden, Paper Th4.4.3.

[5] B. Lankl, J. A. Nossek, and G. Sebald, "Cross-polarization interference cancellation in the presence of delay effects," in *IEEE Proc. ICC 1988*, Philadelphia, PA, Paper 41.4.1-7.

[6] M. Tseytlin, O. Ritterbush, and A. Salamon, "Digital, endless polarization control for polarization multiplexed fiber-optic communications," in *Proc. OFC 2003*, Paper MF83, p. 103.

[7] F. Derr, "Coherent optical QPSK intradyne system: Concept and digital receiver realization," *J. Lightw. Technol.*, vol. 10, no. 9, pp. 1290–1296, Sep. 1992.

[8] S. Norimatsu *et al.*, "Damping factor influence on linewidth requirements for optical PSK coherent detection systems," *J. Lightw. Technol.*, vol. 11, no. 7, pp. 1226–1233, Jul. 1993.

[9] R. Noé, "Phase-noise tolerant feedforward carrier recovery concept for baseband-type synchronous QPSK/BPSK receiver," in *Proc. 3rd IASTED Int. Conf. on Wireless and Optical Communications*, Banff, Canada, Jul. 14–16, 2003, ISBN: 0-88 986-374-1, 197.

[10] ——, "Phase noise tolerant synchronous QPSK receiver concept with digital I&Q baseband processing," in *OECC/COIN 2004*, Yokohama, Japan, Jul. 12–16, 2004, 16C2-5.

[11] R. Noé, E. Meissner, B. Borchert, and H. Rodler, "Direct modulation 565 Mb/s PSK experiment with solitary SL-QW-DFB lasers and novel suppression of the phase transition periods in the carrier recovery," in *ECOC 1992*, vol. 3, Paper Th PD I.5, pp. 867–870.